Modelling one-dimensional insulating materials with the ionic Hubbard model

2005 J. Phys.: Condens. Matter 17 6635

(http://iopscience.iop.org/0953-8984/17/42/004)

INSTITUTE OF PHYSICS PUBLISHING JOURNAL OF PHYSICS: CONDENSED MATTER

J. Phys.: Condens. Matter **17** (2005) 6635–6644 doi:10.1088/0953-8984/17/42/004

Modelling one-dimensional insulating materials with the ionic Hubbard model

M C Refolio, J M Lòpez Sancho and J Rubio

Instituto de Matemàticas y Fìsica Fundamental, CSIC, Serrano 113 bis, E28006 Madrid, Spain

E-mail: refolio@imaff.cfmac.csic.es

Received 30 June 2005, in final form 16 September 2005
Published 7 October 2005
Online at stacks.iop.org/JPhysCM/17/6635

Abstract

The single-particle spectral-weight function of the ionic Hubbard model (IHM) at half-filling shows an abrupt change of regime at a critical value of the coupling constant (Hubbard U). Specifically, this function jumps at the Fermi points $k_F = \pm\pi/2$ from a two-peak to a four-peak structure accompanied by a (non-vanishing) minimum of the single-particle charge gap. This jump separates a weak-coupling regime, the band insulating phase, from a strong-coupling regime which evolves gradually into the Mott–Hubbard phase. We take advantage of this critical behaviour to model several quasi-one-dimensional materials in terms of the IHM instead of the simpler one-band Hubbard model. For instance, the two regimes are physically realized in the angle-resolved photoelectron spectra of $(TaSe_4)_2I$, and the blue-bronze $K_{0.3}MoO_3$, respectively.

1. Introduction

Quasi-one-dimensional (Q1D) systems have been the object of intense experimental and theoretical activity over the last 20 years. They show highly anisotropic properties, with a privileged direction of enhanced charge transport. Their interest lies in the hope that they can be good candidates for the physical realization of non-Fermi liquid behaviour. This interest, in low-D systems in general, has expanded very rapidly in recent years partly due to the technological development of low-D artificial structures and nano-scale materials.

Above their Peierls temperature (or when doped away from half-filling), these Q1D systems are conductors and display Luttinger liquid behaviour [1], i.e., the absence of quasi-particle excitations in the Fermi liquid sense (a quasi-particle peak at the Fermi level) and the excitation, instead, of decoupled collective modes of charge (holons) and spin (spinons) character, a phenomenon usually known as spin–charge separation. The absence of a Fermi edge has indeed been found in angle-resolved photoelectron spectroscopy (ARPES) of $(TaSe_4)_2I$ [2, 3], $K_{0.3}MoO_3$ [4], and the organic conductor TTF–TCNQ (tetrathiafulvalene–tetracyanoquinodimethane) [5, 6]. For a good review, see [7]. Clear experimental signatures of

spin–charge separation are, however, very scarce in Q1D conductors, with the notable exception of TTF–TCNQ reported very recently [6]. All these compounds in their metallic state can be modelled by the low-energy physics of the doped 1D single-band Hubbard Hamiltonian [6]. Alternatively, they have been analysed on the basis of the Luttinger model or the Luther–Emery model (when a spin gap is expected). Some puzzles still remain unsolved [7].

Below their Peierls temperature, these Q1D compounds, as well as many others like halogen-bridged transition-metal chains, conjugated polymers, and organic charge-transfer salts, are usually insulating. In these systems, the competition between strong on-site correlations and their kinetic energy gives rise to significant localization of their itinerant electrons. This often leads to the stabilization of non-metallic ground states with or without charge-density waves (CDWs). Thus $(TaSe_4)_2I$ and the blue-bronze $K_{0.3}MoO_3$, for instance, are CDW insulators [7], while the nearly ideal 1D CuO chains in $SrCuO_2$ and Sr_2CuO_3 are responsible for the insulating character of these charge-transfer insulators [8]. Signatures of spin–charge separation have also been found in ARPES of $SrCuO_2$ [9] and in the dielectric response of Sr_2CuO_3 [10].

Most of these insulating systems can be conveniently described by the Emery model [11], which is a generalized Hubbard Hamiltonian on a two-sublattice model, made of cations (say Cu ions) and anions (say O ions), respectively. The on-site energy levels and repulsions (ϵ_{d}, U_{dd}) and (ϵ_{p}, U_{pp}), for Cu d orbitals and O p orbitals, are coupled by nearest-neighbour hopping of strength t_{dp} and Coulomb repulsions V_{dp}. Its 1D version reads

$$H = \varepsilon_{\mathrm{d}} \sum_{is} n_{\mathrm{d}is} + U_{\mathrm{dd}} \sum_{i} n_{\mathrm{d}i\uparrow} n_{\mathrm{d}i\downarrow} + \varepsilon_{\mathrm{p}} \sum_{js} n_{\mathrm{p}js} + U_{\mathrm{pp}} \sum_{j} n_{\mathrm{p}j\uparrow} n_{\mathrm{p}j\downarrow} + t_{\mathrm{dp}} \sum_{\langle ij\rangle s} (\mathrm{d}^{+}_{is}\mathrm{p}_{js} + \mathrm{hc}) + V_{\mathrm{dp}} \sum_{\langle ij\rangle} n_{\mathrm{d}i} n_{\mathrm{p}j} \tag{1}$$

where d^{+}_{is} creates an electron (hole) in a d orbital at site i with spin s, i running over all the Cu sites. Similarly p_{js} annihilates an electron (hole) in a p orbital at site j and spin s, j running over all the O sites. As usual, $\langle ij\rangle$ means summation over nearest neighbours, $n_s = c^{+}_s c_s$ and $n_i = n_{i\uparrow} + n_{i\downarrow}$ denotes the charge at the ith site.

At first sight the Cu–O repulsion seems essential since a large charge-transfer is expected. However, V_{dp} is usually much smaller than the on-site repulsions and, furthermore, this term gives rise to new physics only in the event of exciton formation. Hence, if we are not especially interested in these processes, V_{dp} can be safely ignored. One is then left with a charge-transfer model Hamiltonian which can still give a reasonable description of some of these compounds [12, 13], e.g., $SrCuO_2$ and Sr_2CuO_3 [7]. If we are now willing to reduce the number of parameters by putting (somewhat arbitrarily) $U_{\mathrm{pp}} = U_{\mathrm{dd}}$, then the so-called ionic Hubbard model (IHM) follows. It can be written simply as

$$H = -t \sum_{\langle ij\rangle s} c^{+}_{is} c_{js} + \frac{\Delta}{2} \sum_{is} (-1)^{i} n_{is} + U \sum_{i} n_{i\uparrow} n_{i\downarrow} \tag{2}$$

where Δ is the on-site energy difference between even and odd sites, usually known as the charge-transfer energy.

Although, again at first sight, this Hamiltonian does not describe accurately any specific system (since quite generally $U_{\mathrm{pp}} < U_{\mathrm{dd}}$), it provides a simple, minimal, model where the interplay among covalency (t), ionicity (Δ) and correlation (U) gives rise to a rich phase diagram within which different 1D compounds can be placed. Originally proposed by Nagaosa and Takimoto [14] as a model for ferroelectric perovskites and later by Egami *et al* [15] to explain the neutral–ionic transition in some organic crystals, this Hamiltonian is ideal for studying the nature of quantum phase transitions in 1D electron systems. On general grounds,

one expects a transition from an ionic, weakly correlated band insulator (BI) phase to a neutral, strongly correlated Mott insulator (MI) phase as U increases. An important and controversial issue is the nature of this transition as well as whether two critical points rather than one separate both phases. Depending on the method of calculation used, either one [16–19] or two [20–23] critical points have been predicted, so the controversy cannot be considered as closed yet.

In this paper we remain outside the above controversy, touching upon it only incidentally. Instead we shall concentrate on the single-particle spectral-weight function (SWF) $A(k, E)$ of this model at half-filling, which can be compared with ARPES of several insulating materials. Somewhat surprisingly, this important quantity for the description of the excitations of an electron system has not received any attention yet in connection with the IHM, all the effort having being concentrated on the nature of the quantum phase transition. $A(k, E)$ will be calculated using the cluster perturbation theory (CPT) approach originally due to Gros and Valenti [24] and more recently reformulated by Senechal *et al* [25]. This is briefly described in section 2. Section 3 describes our results for the critical behaviour of $A(k, E)$ as a function of the Hubbard U, followed by a discussion in section 4 showing that $(TaSe_4)_2I$ and $K_{0.3}MoO_3$ are good qualitative examples of the two phases involved in this critical behaviour. Finally, section 5 closes the paper with some concluding remarks.

2. Cluster perturbation theory

Since this method has been discussed at length in [24] and [25], we simply summarize it very briefly here. In CPT one divides the lattice (here the chain) into a number of equal clusters. The single-particle Green's function (GF) on these clusters is then found by exact diagonalization with open boundary conditions. We have made use of a variant of the Lanczos algorithm specifically designed to calculate dynamic quantities [26]. The approximation now consists in neglecting the intercluster self-energy, so that the GFs of neighbouring clusters are connected by hopping terms only. Periodic boundary conditions are then imposed on the whole chain, i.e., between the extreme clusters. To be specific, let mi denote the site m of the cluster i. The exact Green's function $G_{mi,nj}$, of the whole chain is given by the well-known Dyson's equation in matrix form $(G_0^{-1} - \Sigma)G = I$, in terms of the non-interacting GF and the exact Σ. In CPT this exact Σ is approximated by $\Sigma_{mi,nj} = \delta_{ij}\Sigma^C_{mn}$, where Σ^C is the cluster self-energy matrix. This was, in fact, the original argument of Gros and Valenti [24]. The approximation is applicable to any lattice in any dimension. It can be understood as a lowest-order contribution to a systematic perturbation expansion in powers of the intercluster hopping [25, 27]. It turns out, on the other hand, that CPT is a limiting case of a more general variational cluster approach [28].

In this paper we concentrate on the SWF $A(k, E)$, given as usual by

$$A(k, E) = -\frac{1}{\pi}\,\mathrm{Im}\,G(k, E + \mathrm{i}\eta) \tag{3}$$

where $G(k, E)$ is the Fourier transform (FT) of the single-particle retarded GF and η a positive infinitesimal. This FT must be calculated with some care since $G_{mn}(i - j)$ is periodic in ij but not in mn due to the open boundary conditions used in the clusters. The correct formula is [25, 27]

$$G(k, E) = \frac{1}{N}\sum_{mn} \mathrm{e}^{-\mathrm{i}k(m-n)} G_{mn}(Nk, E) \tag{4}$$

where N is the number of sites in a cluster and $G_{mn}(k)$ the FT of $G_{mn}(i - j)$.

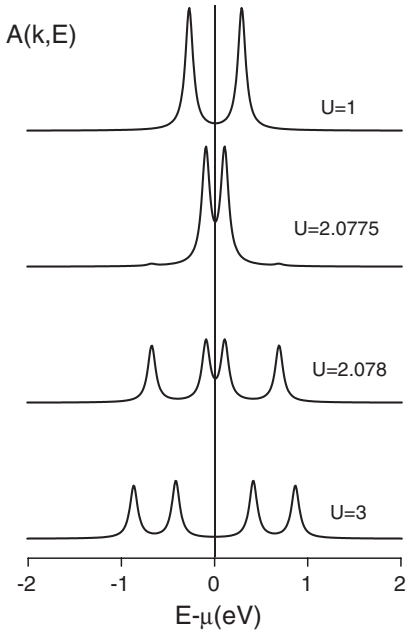

Figure 1. Single-particle spectral-weight function $A(k, E)$ for the half-filled ionic Hubbard model at the Fermi points $k = \pm\pi/2$. From top to bottom, $U = 1$, 2.0775 (just below U_c), 2.078 (just above U_c), and 3. We have taken $t = 1$ and $\Delta = 1$. All the energies are given in eV. The vertical thin line indicates the chemical potential.

In all our calculations we take a chain of 96 sites of two kinds with levels at $\pm\Delta/2$, at half-filling, and take $t = 1$ eV and $\Delta = 1$ eV. Clusters of 8 sites have been adopted after checking that increasing the size of the starting cluster up to 12 sites does not change substantially the results for the whole chain. Some fine structure simply disappears with increasing cluster size (size effects), but the essential features remain almost unaltered.

3. The spectral weight function

Figure 1 shows $A(k, E)$ at the Fermi points $k_F = \pm\pi/2$ for increasing U. A broadening $\eta = 0.05$ eV has been given to the otherwise delta functions. The thin vertical line indicates the chemical potential ($E - \mu = 0$). The two peaks closest to the chemical potential (middle of the gap) delimit the single-particle gap, usually defined by the energy difference between the lowest unoccupied and the highest occupied single particle levels. Two regimes are observed in the low-energy region: for small U, a two-peak structure is seen close to the chemical potential which persists, while the two peaks approach each other, up to $U_1 = 2.0775$ eV. Abruptly, at $U_2 = 2.0780$ eV, a four-peak structure appears, with smaller peaks. This jump can be best understood in terms of the separated-atoms limit and simply signals the ionic-to-neutral transition (recall that the non-interacting dispersion relation vanishes at the Fermi points). In this limit, the ground state jumps from the ionic configuration, with the odd sites doubly occupied and the even sites empty, to the neutral configuration where both even and odd sites are half-occupied. Correspondingly, the one-electron Green's function two-peak to four-peak jump at both the even and odd sites, thus yielding the required two–four peak jump. As U further increases, the SWF tends asymptotically to a Mott–Hubbard

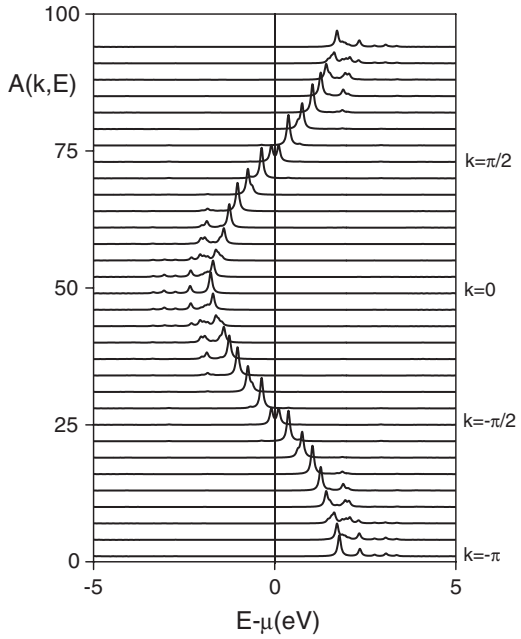

Figure 2. Spectral-weight function $A(k, E)$ of the half-filled IHM for $U = 2.0775$ eV, just below U_c. An offset has been given to the plots for different k s along the large Brillouin zone ($-\pi \leqslant k < \pi$) in order to avoid superposition. The figures along the left vertical axis count the number of k s starting from $-\pi$. On the right vertical axis, some especial k s are indicated. The intersections of the vertical thin with the SWF at $k_F = \pm\pi/2$ mark the middle of the gap.

scenario without any further signature of abrupt change. The single-particle (charge) gap, after passing through a minimum, increases again. It never vanishes, in agreement with recent findings [19, 23].

To check the changes that occurred at $k \neq \pm\pi/2$, figures 2 and 3 display $A(k, E)$ for the values just quoted $U_1 = 2.0775$ eV and $U_2 = 2.0780$ eV, just below and above some intermediate critical U, U_c, along the large Brillouin zone (BZ), $-\pi \leqslant k \leqslant \pi$ (in the extended zone scheme). An offset has been provided to the different plots to avoid superposition. The figures along the left vertical axis number the k s starting from $k = -\pi$ (only a selected set of 32 k s have been shown for clarity). As in figure 1, the thin vertical line indicates the chemical potential. The intersections of this line with the SWF at $k_F = \pm\pi/2$ mark the middle of the gap, which is delimited then by the two adjacent peaks. Figure 2 shows a cosine-like band cut into two pieces (follow the vertical line) by a gap at the Fermi points (cf with the second panel in figure 1). Two shadow bands covering only part of the BZ are clearly visible around $k = 0$ (occupied) and $k = \pi$ (empty). In figure 3, on the other hand, the cosine-like band is now cut by a wider gap delimited by the outer peaks of figure 1, third panel. The inner peaks are continued by two almost non-dispersive, flat bands covering only a small portion of the BZ around k_F. The smaller gap delimited by the inner peaks, i.e., between the flat bands, is the real gap shown by the SWF, continuation of the gap seen in the first regime. In contrast, the Hubbard-like band edges define a wider gap. The system can also be described as having a Hubbard gap with two weakly dispersive, impurity-like peaks close to the middle of the gap, somewhat reminiscent of the lattice-Anderson model. As U increases further, the inner gap increases from its minimum value; the flat bands repel each other and finally merge with the

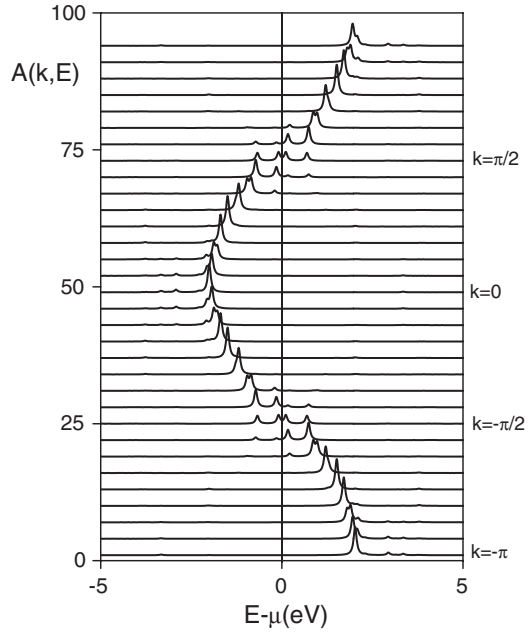

Figure 3. Same as figure 2, but for $U = 2.0780$ eV just above U_c.

Hubbard bands. The system evolves asymptotically onto the Mott–Hubbard phase (infinite U limit). The shadow bands around $k = 0$ and π have now almost disappeared.

The band structures in figures 2 and 3 can be alternatively understood by considering the IHM as a two-component system made up of an electron-doped (the odd sites) and a hole-doped (the *even* sites) system, both slightly away from half-filling. Then the band structure around $k = 0$ is very reminiscent of the hole-doped Hubbard model (a spinon and a holon band). Likewise, the band structure around $k = \pi$ resembles that of the electron-doped Hubbard model, with the same interpretation. Although, as already shown, the physics in the gap region is essentially controlled by the separated atoms limit, a range of k s around k_F also contribute to the DOS (not shown), so that the relative strength of the inner and outer peaks need not be that derived from k_F alone in figure 1.

Summarizing, the two-band structure for $U < U_c$ is continuously connected to the insulator bands at $U = 0$. This is the band insulator (BI) regime. For $U > U_c$, however, we have a strong-coupling regime, more Hubbard-like, which evolves into the Mott–Hubbard regime at large U. This change of regime at U_c is in fact the only signature of a quantum phase transition detected by the single-particle GF. All the E-integrated quantities like the ground-state energy, the ionicity, the double occupancy and the bond charge are *continuous* functions of U, even at U_c, and thus do not provide any hint of a quantum phase transition. This is, for instance, the case of the bond charge, n_{ij}, which is continuous across any single site and therefore tell us nothing about a spontaneous dimerization. To settle this issue one must turn to bond–bond correlations, which have been extensively studied recently by several authors [16, 18–23]. These correlations tell us that our second phase is indeed spontaneously dimerized and therefore the detected transition may correspond to the first critical point of the well-known two-point scenario. The second critical point, associated with the spin gap, cannot be detected by the SWF in a direct way. We wish to stress here that our results are

not in contradiction with those obtained by other authors regarding the nature of quantum phase transitions in the IHM. Simply, quantities like excitation gaps, spin gaps, and bond–bond correlations, are not directly accessible to the single-particle GF. Our results rather add information about a quantum phase transition associated with the *single-particle* gap minimum.

4. Modelling Q1D insulators

The development of high-resolution ARPES in the 1990s revived the interest in Q1D materials. This effort first concentrated on inorganic chain-like materials, like $(TaSe_4)_2I$ and $K_{0.3}MoO_3$, where well characterized, high-quality single crystals were easier to prepare than organic crystals. A further driving force for this effort was to study the opening of large Peierls gaps, which made CDW materials ideally suited for ARPES studies. We concentrate here on these materials and will not pay any further attention to either organic crystals or Mott insulators, also important types of materials.

$(TaSe_4)_2I$ has a chain-like structure leading to a metal–insulator transition to an incommensurate, almost tetramerized, CDW at a Peierls transition temperature $T_p = 263$ K , with an estimated optical or transport gap of 0.25–0.3 eV [29]. The ARPES spectra exhibit a single feature with band-like dispersion throughout the 1D BZ (the ΓX direction) and a complex line shape [2, 3, 30]. The band shows a minimum at Γ, surrounded by maxima near the zone boundaries, but it never comes closer than 0.4 eV to the chemical potential, in contrast with band structure calculations [31] which predict a double crossing of the two 1D, nearly degenerate, Ta 5d conduction bands. The gap persists, essentially unchanged, for higher temperatures well into the normal, metallic phase.

Like $(TaSe_4)_2I$, the molybdenum blue-bronze $K_{0.3}MoO_3$ exhibits 1D electronic properties and a Peierls transition at 180 K to an insulating CDW state with an energy gap of about 100–150 meV. The ARPES data show two spectral features, one dispersing weakly and the other strongly along ΓX (parallel to the chains direction). Both bands have a minimum at Γ and a maximum at X [4, 32, 33]. Neither of them comes closer than 0.18 eV to the chemical potential anywhere in the BZ, in striking contrast to tight-binding calculations [34] which predict two nearly degenerate bands crossing the Fermi level. Any of these calculated bands could fit the shallow experimental band, closer to the chemical potential, but not the second, strongly dispersing band with a bandwidth well above 1 eV. The gap also remains visible at higher temperatures.

The above features, of course, make useless any explanation in terms of the standard Fermi liquid model of metals and semiconductors. Moreover, it seems hard to provide a consistent explanation of them within the framework of any of the simplest, strongly interacting models. For instance, the absence of a Fermi edge in the metallic phase calls for the Luttinger liquid model [1], but the simultaneous presence of a real gap in the low-temperature phase of the above two materials rather hints to the Luther–Emery model [35], where charge transport is compatible with a spin-gapped mode. To attain the required gap sizes, however, one must go to rather unrealistic values of the interaction parameters. These gaps are better described by the fluctuating Peierls insulator model [36], but this model cannot explain the persistence of the gaps above the Peierls temperature.

It is just here where the IHM is more helpful and constitutes a better starting point than, say, the single-band Hubbard model (HM), or any of the above models (which describe some of the low-energy properties of the HM). The IHM is nothing more than a HM generalized for a bipartite lattice with two kinds of sites (anions and cations) with an energy-level difference Δ between them (cf equation (2)). This extra degree of freedom with respect to the HM lends sufficient flexibility to the model for an almost independent determination of both the gap and

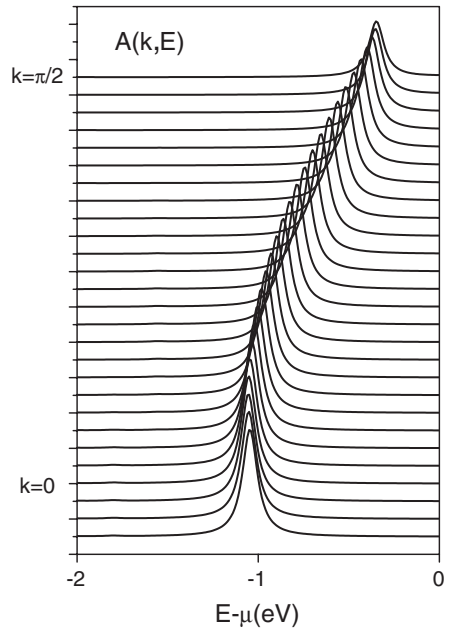

Figure 4. Spectral-weight function for (in eV) $t = 0.5$, $\Delta = 1$ and $U = 0.5$.

other band features. By so doing, the gap is now both of band and many-body origin. As suggested in the introductory section, the interplay among t, U and Δ yields a rich phase diagram within which many Q1D materials can be placed.

The IHM provides a simple explanation of the difference in band structure observed between $(TaSe_4)_2I$ and $K_{0.3}MoO_3$ through the critical behaviour of the single-particle SWF. Thus the first material, with a single band and a large gap, belongs to the BI regime ($U < U_c$) with U lying far below U_c (figure 4). The second material, instead, with two bands and a smaller gap (0.18 eV), must be placed in the strong-coupling ($U > U_c$) regime with U rather close to U_c (figure 5). The figure captions give the parameters used in our calculations. Since both the $(TaSe_4)_2I$ band and the wide band of the blue-bronze have a bandwidth of about 1 eV, we have taken $t = 0.5$ eV. As one can see in figure 5, the flat band described in section 3 (figure 3) simulates the weakly dispersing band of $K_{0.3}MoO_3$. However, it is unclear how this band could proceed all the way from the Fermi surface (X) down to the Γ point.

In any case, an interpretation of the spectral properties of Q1D materials should take into account the discrepancy between the large observed gaps in ARPES and the much smaller gaps related to transport and optical properties. A recent work [37] suggests that the polaronic effects associated to strong electron–phonon interactions may account for these discrepancies, as well as for the asymmetric complex lineshapes of the above materials.

5. Conclusions

Using the cluster perturbation theory approach we have calculated the single-particle spectral-weight function $A(k, E)$ of the ionic 1D Hubbard model at half-filling. A change of regime is found at a critical value of U, $U_c(t, \Delta)$, which depends on both the hopping amplitude t and the on-site energy difference, Δ, between even and odd sites. As U increases, $A(k, E)$ jumps from a two-peak structure to a four-peak one at the Fermi points $k_F = \pm\pi/2$. As one

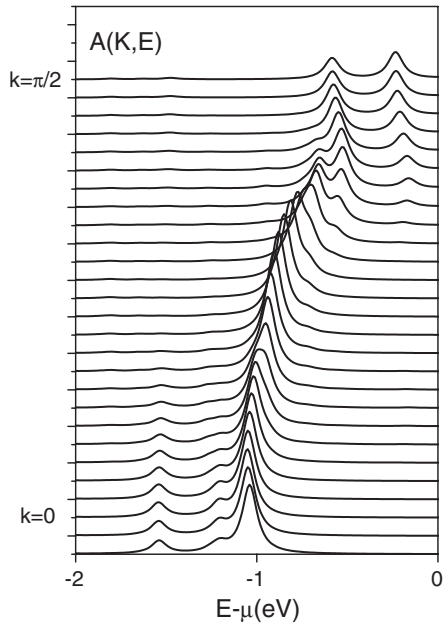

Figure 5. The same as figure 4, but for $U = 2.1$ eV.

moves away from k_F, two semiconducting bands are found for $U < U_c$, separated by a gap which decreases from its initial value Δ (at $U = 0$) down to a small, but non-vanishing, value at U_c. This gap is always delimited by the two-peak structure at k_F. For $U > U_c$, instead, two flat, almost-non-dispersive bands appear around the Fermi points inside the gap between the two Hubbard-like bands. As U increases further, the flat bands approach the Hubbard bands, finally merging into them. Asymptotically, a Mott–Hubbard phase is approached gradually without any signature of abrupt change in $A(k, E)$ along this region of large U.

The two CDW insulators $(TaSe_4)_2I$ and $K_{0.3}MoO_3$ are good examples of qualitative behaviour according with these regimes. They can be placed, respectively, within the first, BI regime (a single occupied band) and the second, strong-coupling regime (two occupied bands)

Acknowledgment

We acknowledge the financial support of the Spanish DGICYT through Project BFM 2002-01594.

References

[1] Haldane F D M 1981 *J. Phys. C: Solid State Phys.* **14** 2585
[2] Hwu Y, Alméras P, Marsi M, Berger H, Lévy F, Grioni M, Malterre D and Margaritondo G 1992 *Phys. Rev.* B **46** 13624
[3] Terrasi A, Marsi M, Berger H, Margaritondo G, Kelley R J and Onellion M 1995 *Phys. Rev.* B **52** 5592
[4] Gweon G H, Denlinger J D, Allen J W, Claesson R, Olson C G, Höchst H, Marcus J, Schlenker C and Schneemeyer L F 2001 *J. Electron Spectrosc. Relat. Phenom.* **117/118** 481
[5] Zwick F, Jerome D, Margaritondo G, Onellion M, Voit J and Grioni M 1998 *Phys. Rev. Lett.* **81** 2974
[6] Sing M, Schwingenschlogl U, Claesson R, Blaha P, Carmelo J M P, Martelo L M, Sacramento P D, Dressel M and Jacobsen C S 2003 *Phys. Rev.* B **68** 125111

[7] Grioni M and Voit J 2000 *Electron Spectroscopies Applied to Low-Dimensional Materials* vol 1, ed H Starnberg and H Hughes (Dordrecht: Kluwer)
[8] Penc K and Stephan W 2000 *Phys. Rev.* B **62** 12707
[9] Kim C, Matsuura A Y, Shen Z-X, Motoyama N, Eisaki H, Uchida S, Tohyama T and Maekawa S 1996 *Phys. Rev. Lett.* **77** 4054
[10] Neudert R, Knupfer M, Golden M S, Fink J, Stephan W, Penc K, Motoyama N, Eisaki H and Uchida S 1998 *Phys. Rev. Lett.* **81** 657
[11] Emery V J 1987 *Phys. Rev. Lett.* **58** 2794
[12] Zanen J, Sawatzky G A and Allen J W 1985 *Phys. Rev. Lett.* **55** 418
[13] Meinders M B, Eskes H and Sawatzky G A 1993 *Phys. Rev.* B **48** 3916
[14] Nagaosa N and Takimoto J 1986 *J. Phys. Soc. Japan* **55** 2735
[15] Egami T, Ishihara S and Tachiki M 1993 *Science* **261** 1307
[16] Resta R and Sorella S 1995 *Phys. Rev. Lett.* **74** 4738
[17] Gidopoulos N, Sorella S and Tosatti E 2000 *Eur. Phys. J.* B **14** 217
[18] Wilkens T and Martin R M 2001 *Phys. Rev.* B **63** 235108
[19] Kampf A P, Sekania M, Japaridze G I and Brune Ph 2003 *J. Phys.: Condens. Matter* **15** 5895
[20] Fabrizio M, Gogolin A and Nersesyan A A 1999 *Phys. Rev. Lett.* **83** 2014
[21] Takada Y and Kido M 2001 *J. Phys. Soc. Japan* **70** 21
[22] Zhang Y Z, Wu C O and Lin H Q 2003 *Phys. Rev.* B **67** 205109
[23] Manmana S R, Meden V, Noack R M and Schonhammer K 2004 *Phys. Rev. Lett.* **70** 155115
[24] Gros C and Valenti R 1994 *Ann. Phys., Lpz.* **3** 460
[25] Senechal D, Perez D and Pioro-Ladriere M 2000 *Phys. Rev. Lett.* **84** 522
[26] Dagotto E 1994 *Rev. Mod. Phys.* **66** 763
[27] Senechal D, Perez D and Plouffe D 2002 *Phys. Rev.* B **66** 075129
[28] Potthoff M, Aichhorn M and Dahnken C 2003 *Phys. Rev. Lett.* **91** 206
[29] Grüner G 1994 *Density Waves in Solids* (Reading, MA: Addison-Wesley)
[30] Claessen R, Wilde C, Reinert F, Hüfner S, Gweon G-H, Allen J W, Poirier D M and Olson C G 1997 *Phys. Rev.* B **56** 12643
[31] Gressier P, Whangbo M-H, Meerschaut A and Rouxel J 1984 *Inorg. Chem.* **21** 1221
[32] Claessn R, Gweon G-H, Reinert F, Allen J W, Ellis W P, Shen Z-H, Olson C G, Schneemeyer L F and Levy F 1995 *J. Electron Spectrosc. Relat. Phenom.* **76** 121
[33] Gweon G-H, Allen J W, Claessen R, Clack J A, Poirier D M, Benning P I, Olson C G, Ellis W P, Zhang Y-X, Schneemeyer L F, Marcus J and Schlenker C 1995 *J. Phys.: Condens. Matter* **8** 9923
[34] Whangbo M H and Schneemeyer L F 1986 *Inorg. Chem.* **25** 2424
[35] Luther A and Emery V J 1974 *Phys. Rev. Lett.* **33** 589
[36] Lee P A, Rice T M and Anderson P W 1973 *Phys. Rev. Lett.* **31** 462
[37] Perfetti L, Berger H, Reginelli A, Degiorgi L, Höchst H, Voit J, Margaritondo G and Grioni M 2001 *Phys. Rev. Lett.* **87** 216404